OMTM, Volume *8*

Supplemental Information

Enhanced Expression of Anti-CD19 Chimeric Antigen Receptor in *piggyBac* Transposon-Engineered T Cells

Daisuke Morita, Nobuhiro Nishio, Shoji Saito, Miyuki Tanaka, Nozomu Kawashima, Yusuke Okuno, Satoshi Suzuki, Kazuyuki Matsuda, Yasuhiro Maeda, Matthew H. Wilson, Gianpietro Dotti, Cliona M. Rooney, Yoshiyuki Takahashi, and Yozo Nakazawa

Supplemental Figures and Legends

Figure S1

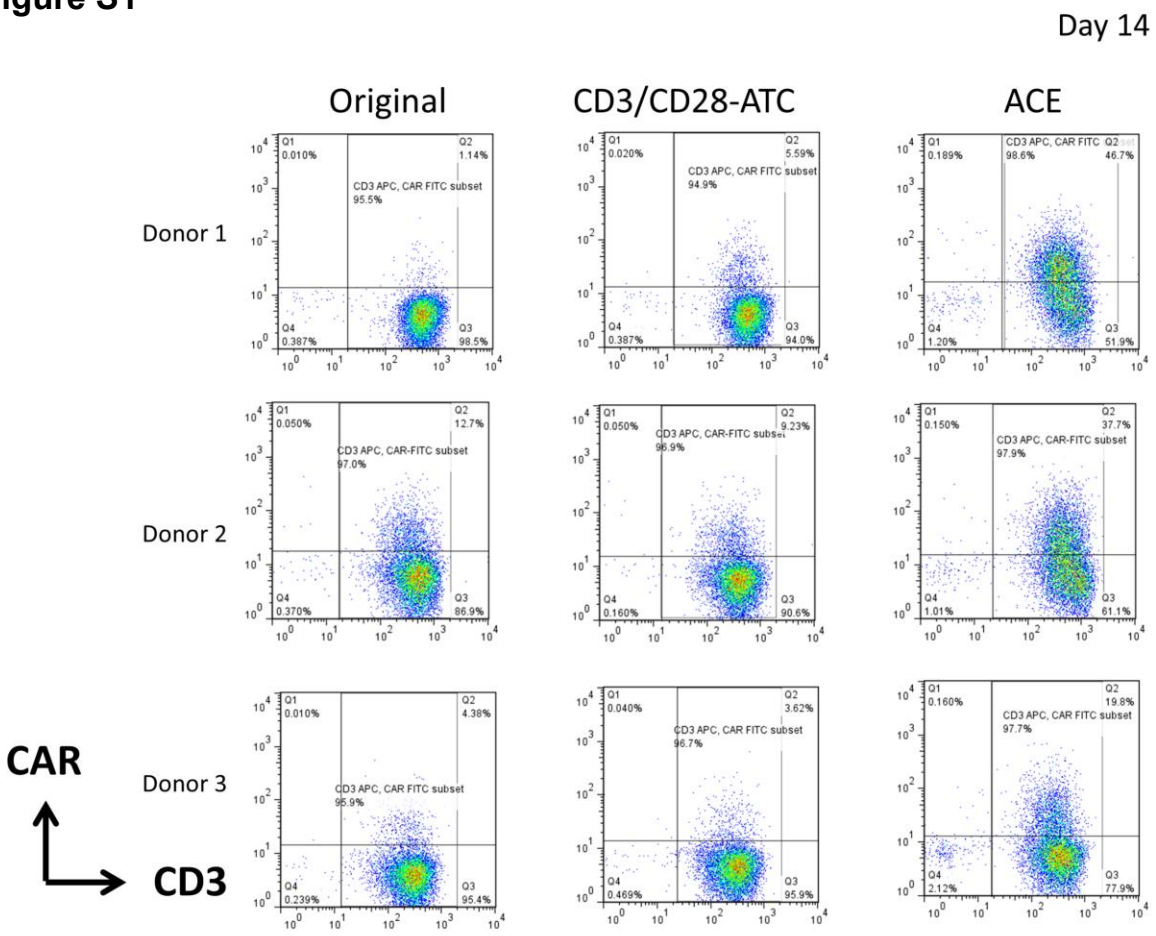

Figure S1. The CAR expression of CD19.CAR-T cells by original, CD3/CD28-ATC, and ACE method. CD19.CAR-T cells were harvested on day 14 and analyzed by flow cytometry. The Figure shows representative dot plots of CD3/CAR expressions generated by either original, CD3/CD28-ATC, or ACE method from 3 healthy donors.

Figure S2

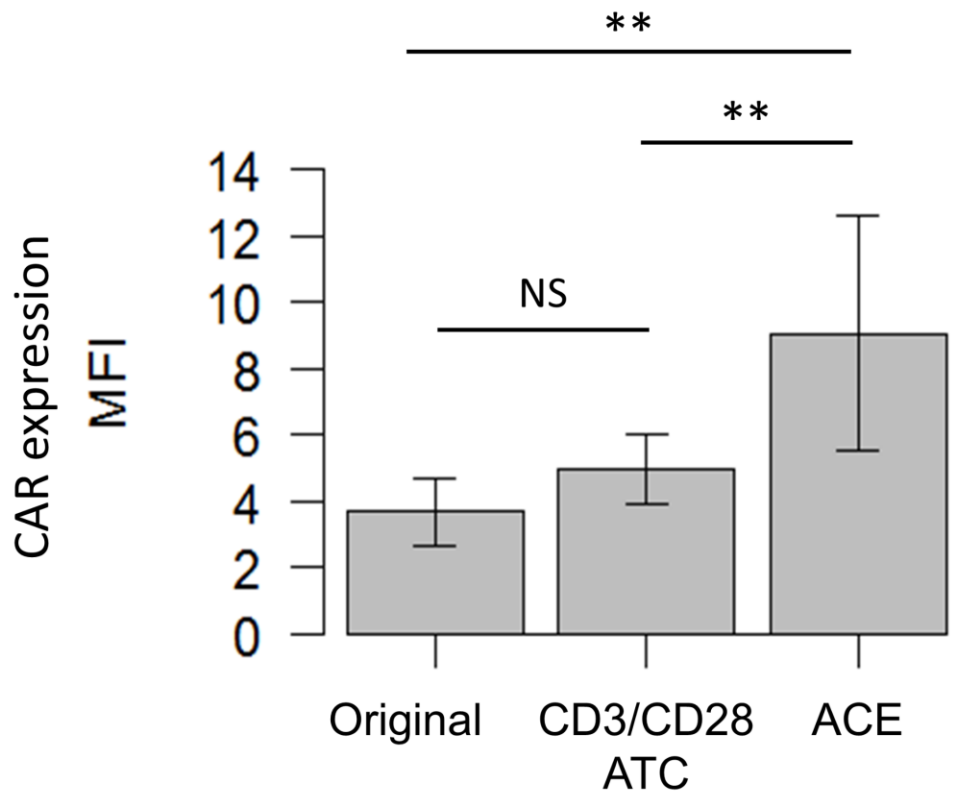

Figure S2. Summarized results of MFI of the CAR expression of CD19.CAR-T cells by original, CD3/CD28-ATC, and ACE method. CD19.CAR-T cells were harvested on day 14 and analyzed by flow cytometry. The figure shows mean fluorescence intensity ± SD of CAR expressions in CAR-T cells generated by either original, CD3/CD28-ATC, or ACE method from 9 donors. NS, not significant; **, $P < 0.01$.

Figure S3

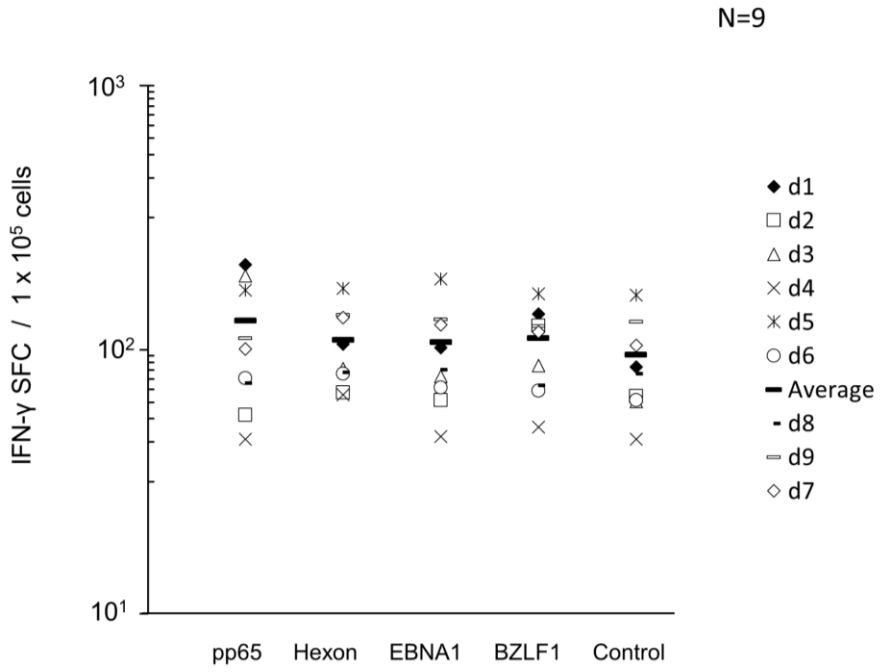

Figure S3. The virus specificity in ACE CD19.CAR-T cells. The virus specificity was analyzed in ACE CD19.CAR-T cells on day 14. Accordingly, 1×10^5 ACE CD19.CAR-T cells were stimulated by each of the four viral antigens (i.e., pp65, Hexon, EBNA1, and BZLF1) or medium alone (control). After 20 hours of incubation, specific IFN-γ secretion by ACE CAR-T cells was assessed by the ELISpot assay. The figure summarizes the results of 9 healthy donors.

Figure S4

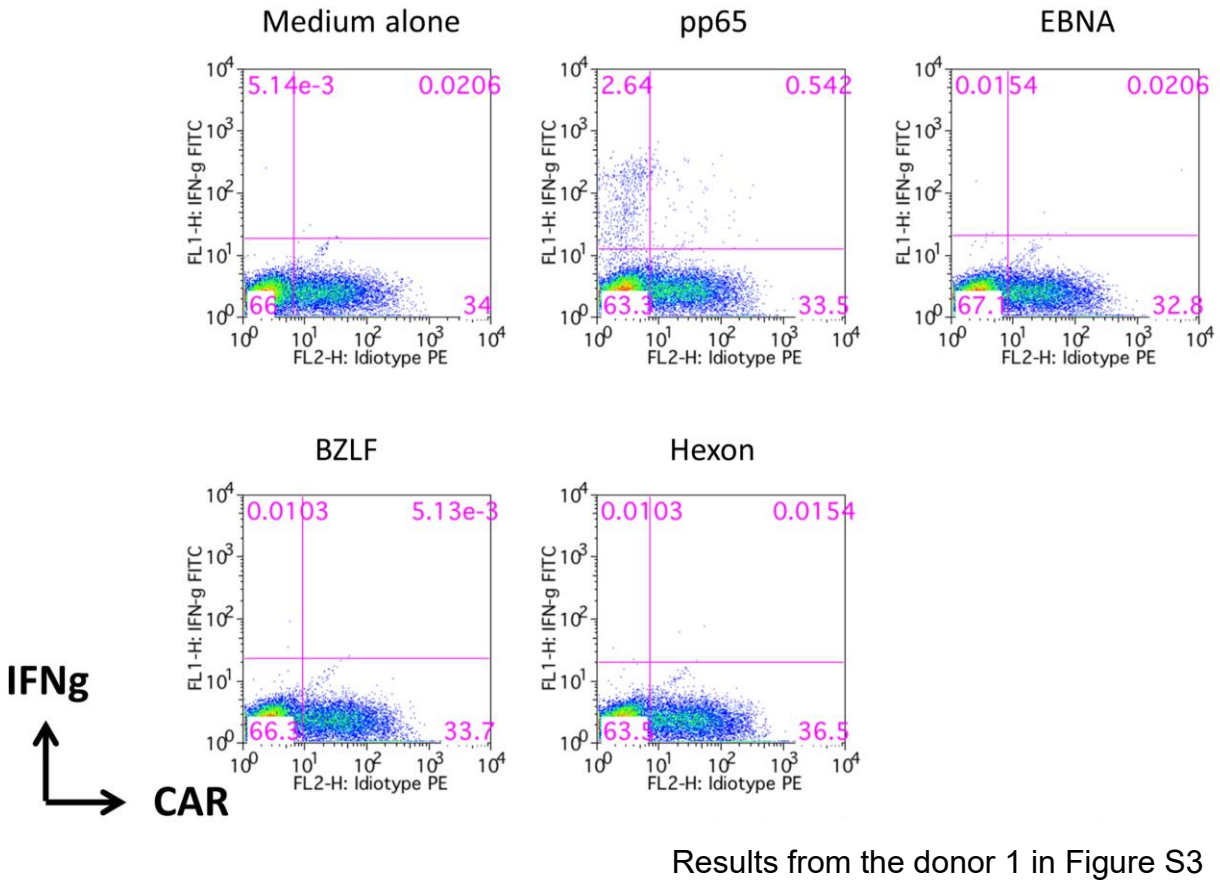

Figure S4. The intracellular cytokine assay of ACE CAR-T cells that retained the virus specificity on day 14. The intracellular staining of IFN-γ was analyzed in ACE CD19.CAR-T cells from donor 1 who retained the virus specificity on day 14. Surface staining of CAR was performed before the intracellular staining. Intracellular synthesis of IFN-γ in response to each viral peptide or medium alone was analyzed by flow cytometry. The result of donor 1 was shown.

Figure S5

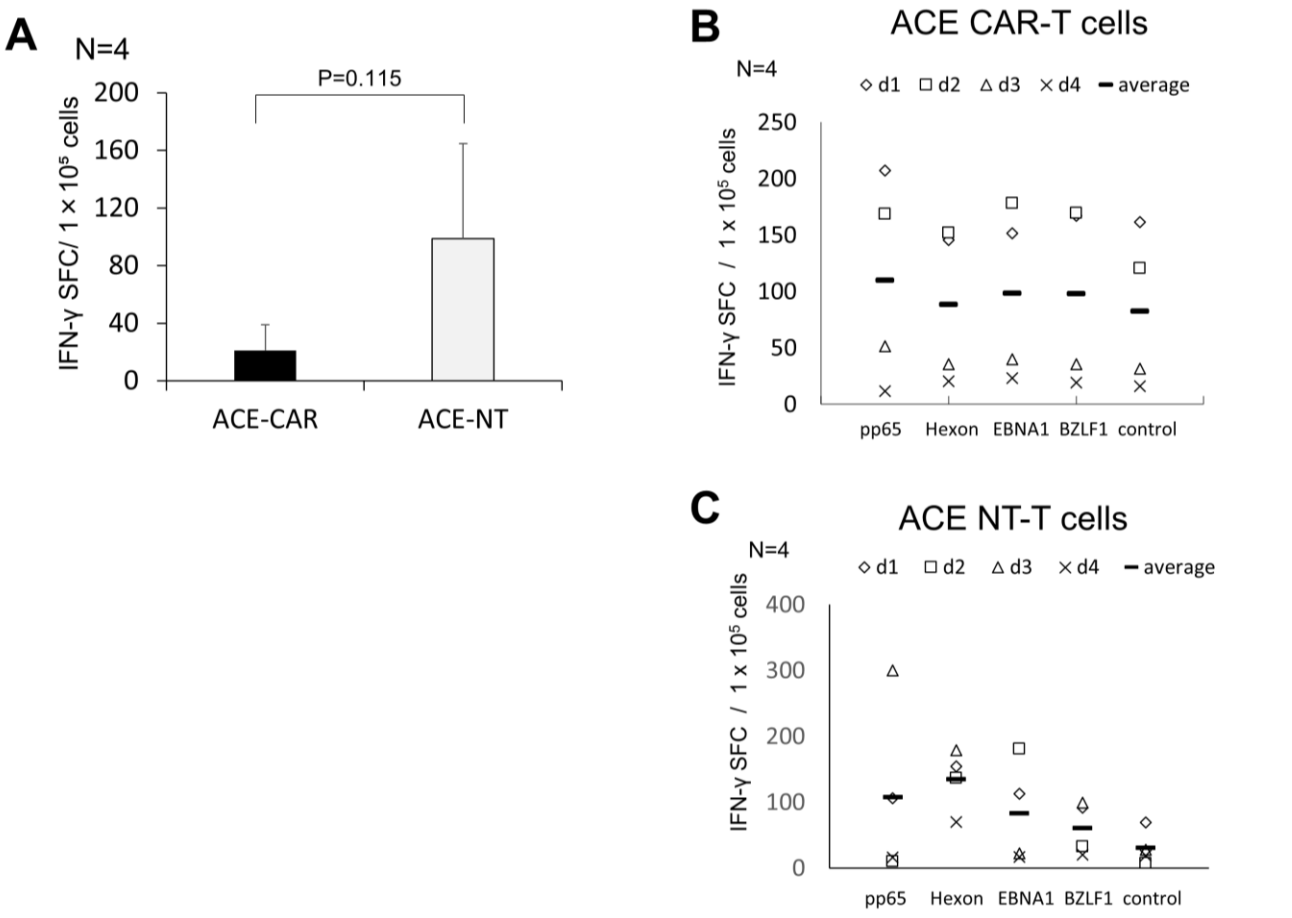

Figure S5. A comparison of the virus specificity between CAR-transduced and NT T cells stimulated by ACE viral peptides. The virus specificity was analyzed in ACE CD19.CAR-T cells or ACE NT-T cells on day 14. In addition, IFN-γ secretion in response to the four viral antigens (Hexon, pp65, EBNA1, and BZLF1) or medium alone (control) was measured by the ELISpot assay. (A) Summarized results of the virus specificity of either CAR-transduced or NT ACE T cells. It shows mean ± SD of the results obtained from 4 healthy donors. The numbers of spots in the negative controls were subtracted from the results. (B) Specific IFN-γ secretion in response to each viral peptide by ACE CAR-T cells. (C) Specific IFN-γ secretion in response to each viral peptide by NT CAR-T cells.

Figure S6

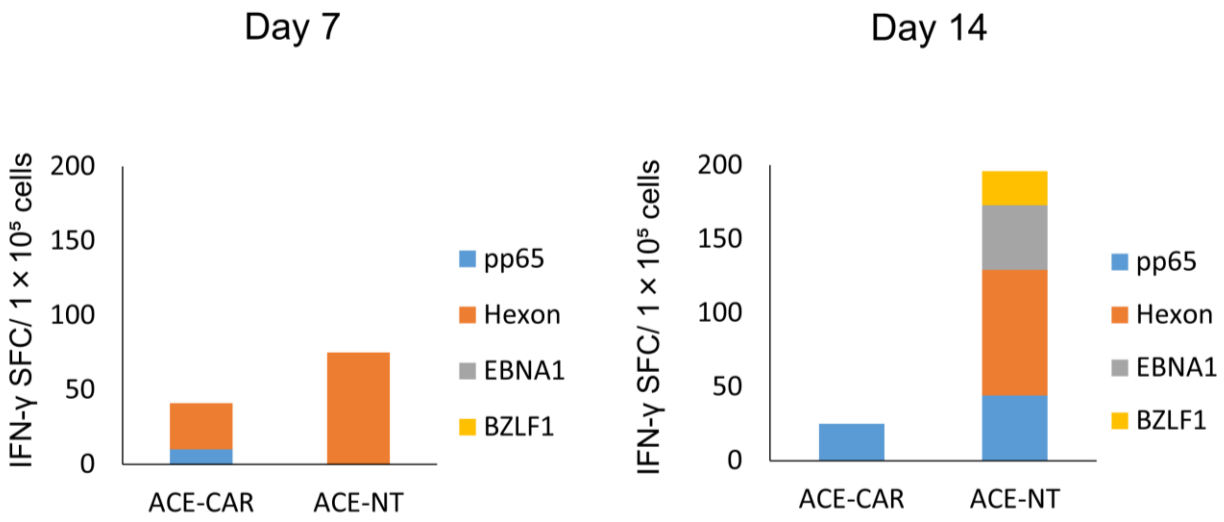

Figure S6. ACE CAR-T cells maintained the virus specificity by day 7 but lost their virus-specific activities by day 14. The virus specificity was sequentially analyzed in either ACE CD19.CAR-T cells or ACE NT-T cells on days 7 and 14. IFN-γ secretion in response to the four viral antigens (i.e., pp65, Hexon, EBNA1, and BZLF1) or medium alone (control) was measured by the ELISpot assay. The figure shows the result of 1 healthy donors. The numbers of spots in the negative controls were subtracted from the results.

Figure S7

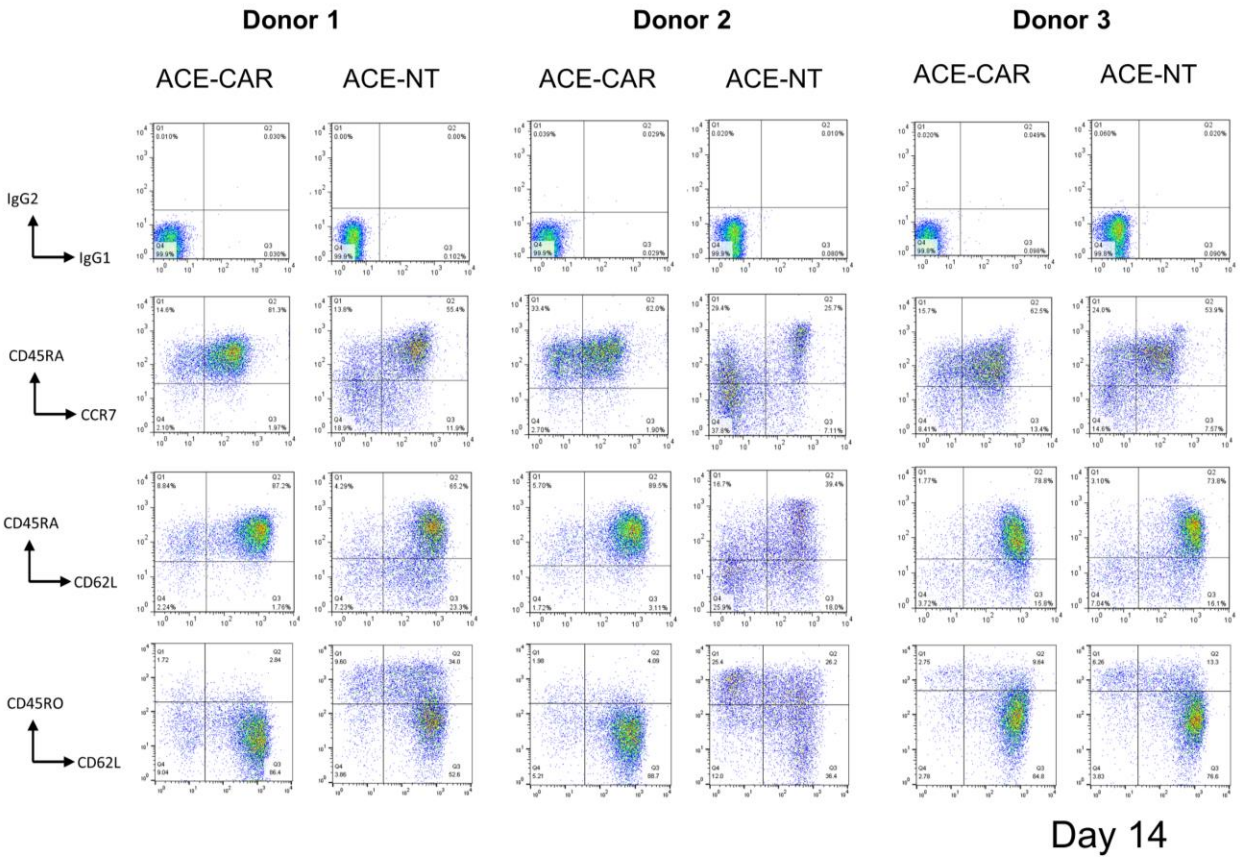

Figure S7. A comparison of phenotype analysis between CAR-transduced and NT ACE T cells.

The phenotypical analysis of either CAR- or NT-ACE CAR-T cells was performed on day 14 after nucleofection. The figure shows representative dot plots of isotype control, CD45RA/CCR7, CD45RA/CD62L, and CD45RO/CD62L from 3 donors.

Figure S8

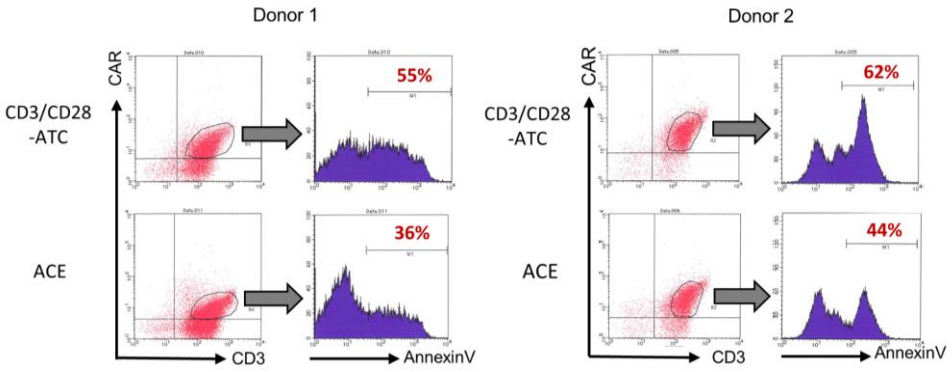

Figure S8. Stimulation with CD3/CD28 mAbs induced apoptosis in PB-modified CAR-expressing T cells.

CD19.CAR transfected cells were stimulated with either viral peptides (ACE) or CD3/CD28 mAbs (CD3/CD28-ATC), then harvested, and analyzed by flow cytometry on day 7 post-stimulation. Annexin V expression was examined within the $CD3^{+}CAR^{+}$ cells. The flow cytometry results of 2 donors are shown.

Figure S9

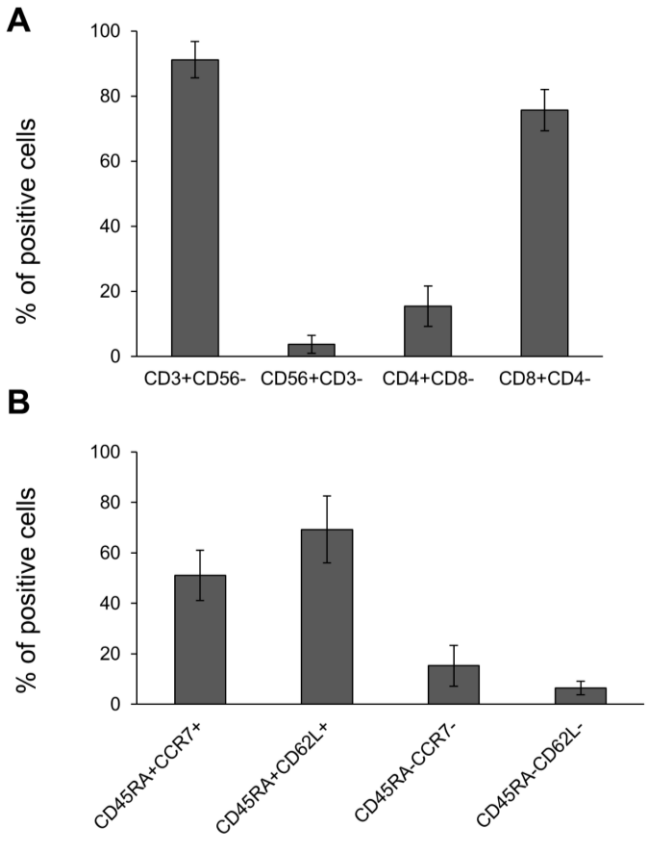

Figure S9. The major subset of ACE CAR-T cells using the CH2CH3-free transposon vector was phenotypically $CD8^+CD45RA^+CCR7^+$.

(A) The phenotypical analysis of ACE CAR-T cells using the CH2CH3-free vector was performed on day 14 after nucleofection. The figure shows the mean expression ± SD in ACE CAR-T cells generated from 9 donors on $CD3^+CD56^-$, $CD56^+CD3^-$, $CD4^+CD8^-$, and $CD8^+CD4^-$ (A), or on $CD45RA^+CCR7^+$, $CD45RA^+CD62L^+$, $CD45RA^-CCR7^-$, and $CD45RA^-CD62L^-$ (B).

Figure S10

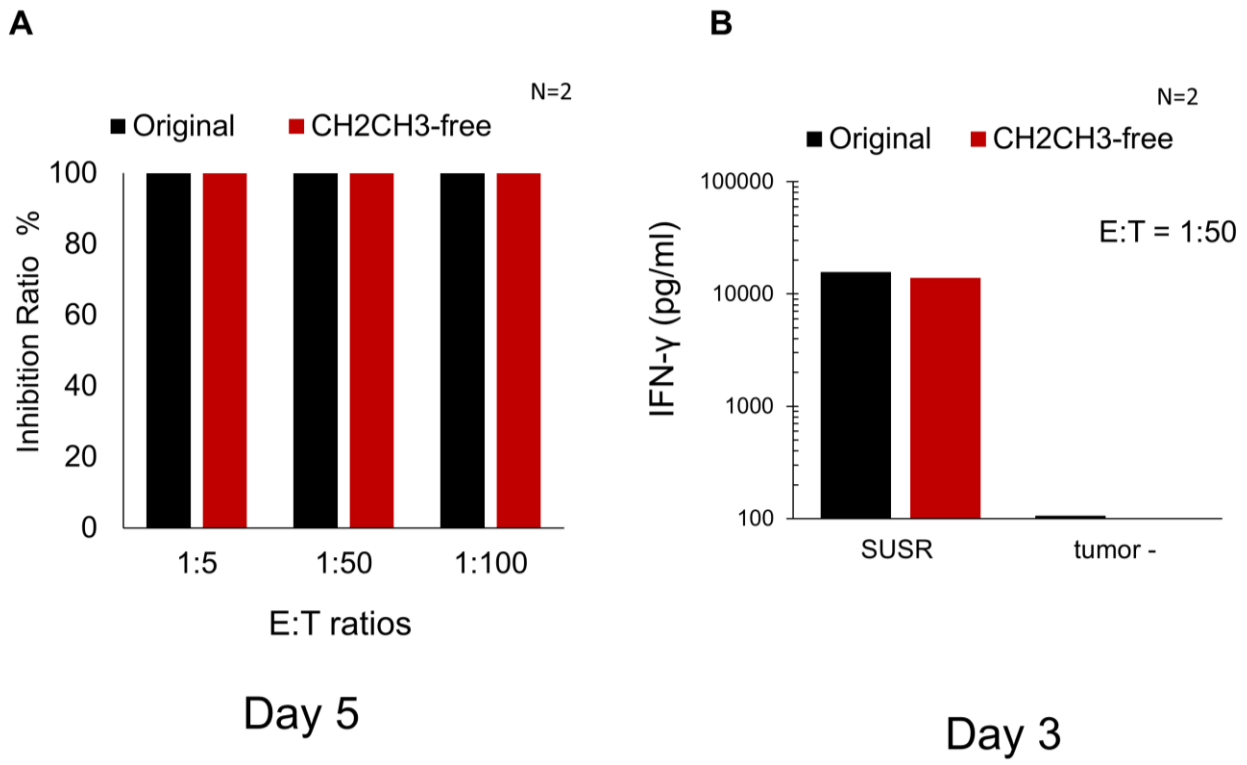

Figure S10. ACE CD19.CAR using CH2CH3-free transposon vector demonstrated a comparable *in vitro* activity. ACE CD19.CAR-T cells with either original or CH2CH3-free transposon vector were co-cultured with $CD19^+$ tumor cells (SU/SR) at effector: target (E:T) ratios of 1:5, 1:50, and 1:100 without cytokines for 5 days. (A) The number of viable cells was determined using a trypan blue exclusion test, and the percentages of T cells and $CD19^+$ cells were determined by flow cytometry. Inhibition ratio was calculated by dividing the input $CD19^+$ cell number by the $CD19^+$ cell numbers in tumor only condition. (B) Data are presented as the mean ± SD of experiments from 2 donors. IFN-γ secretion by ACE CAR-T cells was measured in response to $CD19^+$ tumor cells (SU/SR) at E*T ratios of 1:50 on day 3 after co-culture.